

New Techniques for the Assessment of Regional Left Ventricular Wall Motion

Miguel Angel Garcia-Fernandez, M.D.,* Javier Bermejo, M.D.,* Esther Perez-David, M.D.,* Teresa Lopez-Fernandez, M.D.,* Maria Jesus Ledesma, M.S.Eng.,† Pio Caso, M.D.,§ Norberto Malpica, M.S.Eng.,‡ Andres Santos, Ph.D.,‡ Mar Moreno, M.D.,* and Manuel Desco, M.D., Ph.D.†

*Cardiac Imaging Laboratory, Department of Cardiology and †Department of Experimental Medicine, Hospital Universitario Gregorio Marañón, Madrid, Spain; ‡Escuela Tecnica Superior de Telecomunicaciones, Universidad Politécnica de Madrid, Spain; and §Hospitale Monaldi, Naples, Italy

The assessment of regional left ventricular (LV) function has been an important yet unresolved problem since the introduction of echocardiography as a diagnostic tool. Abnormal regional LV wall motion is an early finding in multiple cardiac pathologies and its diagnosis is of critical importance. In the last few years diagnostic procedures based on combined use of existing echocardiographic technologies were geared toward improving the accuracy of detection of baseline and/or induced regional wall motion abnormalities. One of the assumptions is that the combination of reduced LV wall thickening and reduced myocardial velocities can be used to accurately diagnose regional myocardial dysfunction. In this article we will discuss several new techniques for the quantification of regional LV function using Doppler echocardiography. (ECHOCARDIOGRAPHY, Volume 20, October 2003)

ventricular function, wall motion, myocardial velocity, Doppler

Pulsed Doppler Myocardial Imaging

Pulsed-wave Doppler tissue imaging (DTI) can be used to investigate the systolic phase of each single myocardial wall segment. In normal patients, peak systolic velocity measured in the four-chamber view decreases from base to apex. Previous studies described direct correlation between ejection fraction (EF) and peak systolic myocardial velocity ($r = 0.80$), and inverse correlation between EF and time from ECG Q-wave to peak systolic myocardial velocity ($r = -0.75$).^{1,2}

Myocardial systolic function has been evaluated by pulsed-wave DTI in several types of cardiomyopathy. In patients with dilated cardiomyopathy, a decrease in systolic myocardial velocity was noted along both long and short axes. All systolic DTI variables, particularly peak systolic myocardial velocity along the long axis, correlated well with

peak dP/dt .^{3,4} In systemic amyloidosis, regional myocardial dysfunction can also be depicted in patients with normal ejection fraction, revealing a progressive decrease in peak systolic myocardial velocities from cardiac amyloidosis to cardiac amyloidosis with heart failure.⁵

Pulsed-wave DTI analysis of systolic function is also useful for differentiating between pathologic and physiologic LV hypertrophy, which is reflected by a decrease in mean systolic annular velocity < 9 cm/sec (sensitivity 87%, specificity 97%).⁶ In high performance athletes, systolic velocity of the basal interventricular septum is increased and is positively correlated with septal thickness, suggesting that the septum greatly contributes to the longitudinal LV systolic shortening.^{7,8}

During acute ischemia, characteristic changes can be seen in both systole and diastole. A typical ischemic pattern is a combination of reduced systolic velocity, increased delay from electrocardiogram (ECG) Q-wave to peak systolic myocardial velocity, and the presence of postsystolic thickening reflected by a positive wave in viable tissue that appears after aortic valve closure (Fig. 1).

Address for correspondence and reprint requests: Miguel Angel Garcia-Fernandez, M.D., Servicio de Cardiología No Invasiva, Laboratorio de Ecocardiografía, Hospital General Universitario "Gregorio Marañón," Calle Doctor Esquerdo 46, Madrid 28007, Spain. Fax: +34 (91) 586 8018; E-mail: magfeco@seker.es

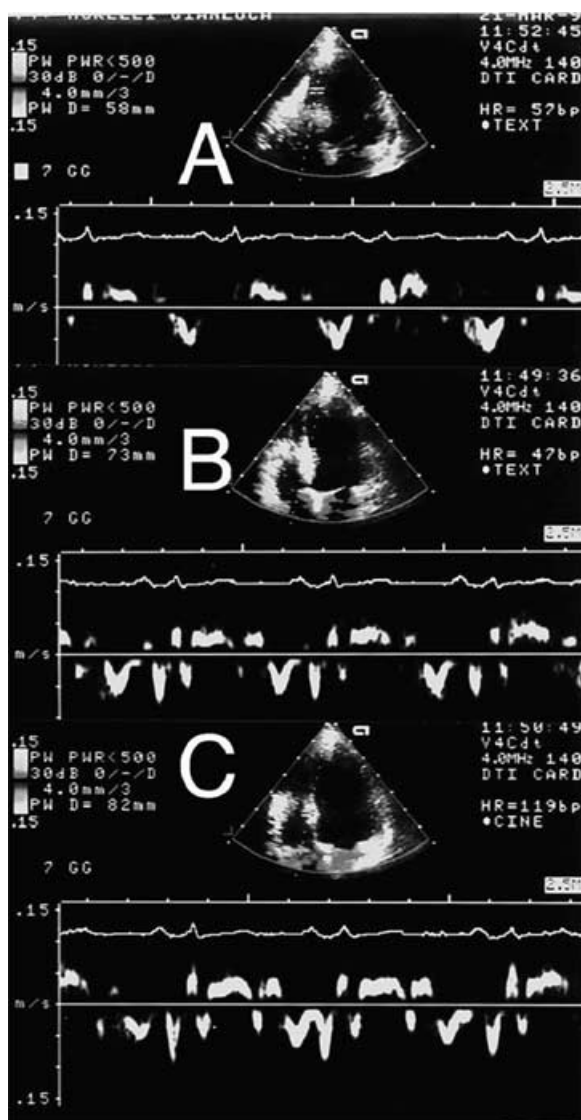


Figure 1. Apical infarction illustrating pulsed-wave Doppler tissue imaging of (A) apical septum, (B) mid-septum, and (C) basal posterior septum. Note that in the apical segment during systole only passive motion is evident. In the middle segment, a marked reduction in systolic motion is accompanied by postsystolic thickening.

In patients with known or suspected coronary artery disease, analysis of systolic regional function has also been proposed as a way to quantify dobutamine echocardiographic data. In response to dobutamine, ischemic segments were found to exhibit the lowest increase in systolic peak velocities. The sensitivity and specificity of DTI for detection of ischemia was 86% and 96% for basal segments using a peak sys-

tolic myocardial velocity of < 12 cm/sec as an indicator of an abnormal response.⁹ DTI of asynergic myocardium during dobutamine stress echocardiography can also be used to quantitatively identify viable myocardium. Assuming 35% increase in systolic myocardial velocity velocities caused by dobutamine as a cutoff for viability, 89% sensitivity and 86% specificity were achieved for predicting postrevascularization functional recovery.¹⁰

Doppler tissue imaging is also a useful tool in assessing the severity of LV asynchrony in patients with left bundle branch block (LBBB) and heart failure, as well as in evaluating the effects of pacing on long-axis function (Fig. 2). Recent studies evaluated the effects of biventricular pacing on myocardial activation delay in patients with advanced heart failure and wide ECG complexes.^{11,12}

One of the main technical limitations of pulsed-wave DTI in the evaluation of regional LV function is that velocity values are strongly affected by the angle between the Doppler sample and the dominant wall motion vector in each specific myocardial segment. This limitation makes the quantification of regional LV function using pulsed-wave DTI impractical for routine clinical work.¹³

Color M-Mode Doppler Tissue Imaging

Color M-mode allows the quantification of myocardial velocities at different depths of the myocardial wall and velocity differences across the myocardium. These differences are assessed by calculating myocardial velocity gradients. Thus, color M-mode is the first echocardiographic tool to provide direct insight into myocardial function (Fig. 3). Such analysis of myocardial function may be especially important in conditions that affect myocardial function in a nonhomogeneous way, such as ischemic heart disease.

Compared with pulsed-wave DTI, color M-mode DTI provides less information for an individual pixel. On the other hand, the entire myocardial wall can be analyzed simultaneously with color M-mode, whereas pulsed DTI is only able to evaluate a relatively small sample volume. The main drawback of this technique compared with other DTI modalities is the impossibility of obtaining reliable measurements from all cardiac segments, because velocity obtained from M-mode is only accurate when the ultrasound beam is perpendicular to the muscle fibers. For this reason color M-mode

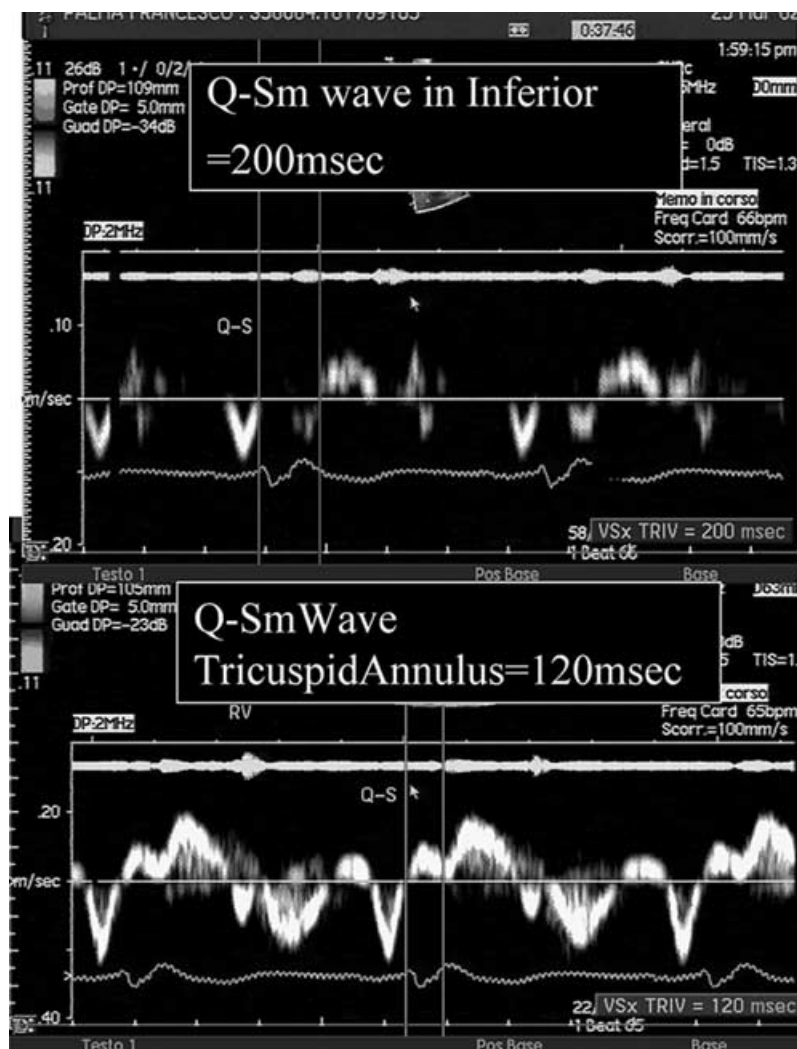


Figure 2. The use of pulsed-wave Doppler tissue imaging to select patients for resynchronization therapy is depicted. In this example, obtained in a patient with dilated cardiomyopathy and left bundle branch block, note the interventricular delay of 80 msec. This delay is reflected by the difference in the time interval from electrocardiogram Q-wave to peak systolic myocardial velocity (S_m) measured at the tricuspid annulus and at the inferior wall, which was the most delayed in this patient.

measurements are generally performed from the parasternal views, in the anterior septum and basal posterior walls, where this requirement is best met.

In a normally contracting heart, systolic LV wall thickening is nonuniform. Maximal rate of systolic thickening is known to be higher near the endocardium than the epicardium.¹⁴⁻¹⁸ The mathematical definition of velocity gradient is velocity difference per unit distance. DTI is sensitive enough to detect these differences across the myocardium during contraction as well as relaxation in protodiastole.¹⁹⁻²¹ Therefore, a myocardial velocity gradient (MVG) can be calculated from color M-mode DTI at any phase of the cardiac cycle, and it appears as a useful parameter for the evaluation of regional myocardial function. Different ways of calculat-

ing myocardial velocity gradient in DTI studies have been proposed. Fleming and associates²² suggested estimating it through linear regression of the velocities across the wall. Assuming that velocity gradients are linear in the myocardium, velocity gradient is defined as the slope of the line through the velocity estimates across the myocardial wall. It may also be calculated in a simplified way as the difference in myocardial velocity between the endocardium and epicardium divided by the myocardial wall thickness.²³

Another strategy to study intramyocardial function is to define different layers of the myocardial wall in order to obtain independent quantitative analysis of each layer.²⁴ Similar to the calculation of MVGs, this technique requires image postprocessing.⁶ Multilayer

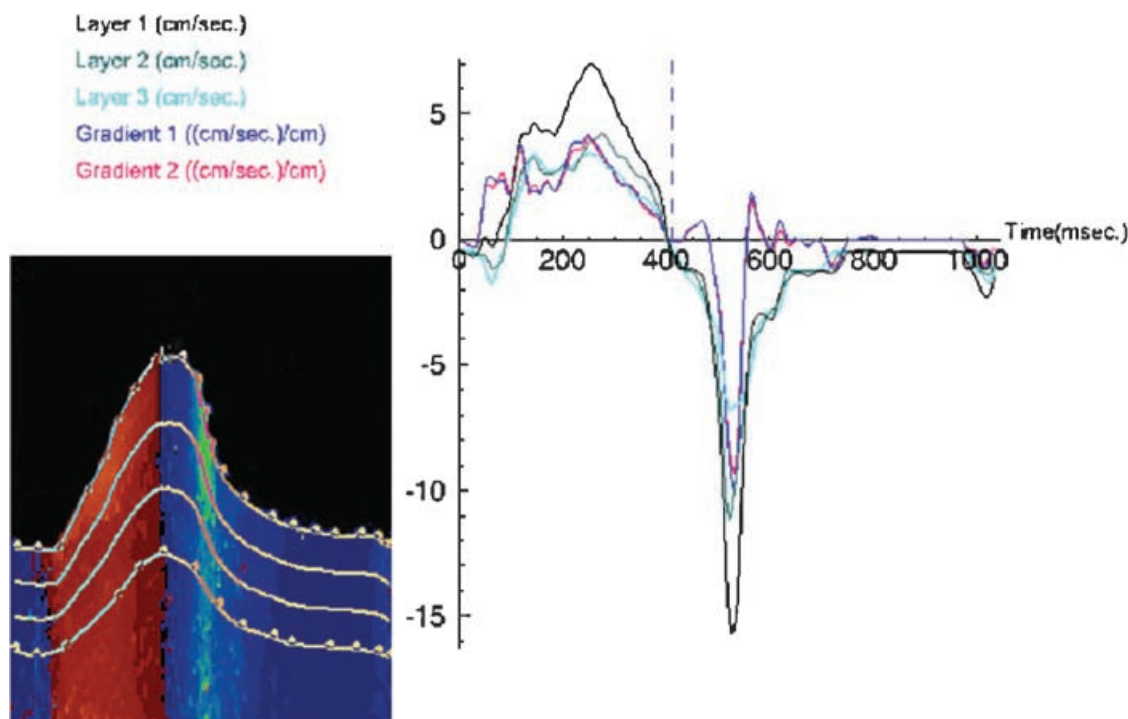


Figure 3. Color M-mode multilayer Doppler tissue imaging (DTI) obtained in a healthy 29-year-old volunteer (left) and analysis results (right). The analysis included semiautomatic tracing of the endocardial and epicardial boundaries on an averaged gray-scale image (not shown), followed by dividing the myocardium into three layers, in which myocardial velocities and velocity gradients are automatically calculated. The dotted line marks end systole, or the point where red color in the DTI image turns blue. Note the positive values in systole and negative values in diastole in the velocity plot. Early and late nadir represent early relaxation and atrial emptying, respectively.

myocardial velocities can provide complementary information to velocity gradients because gradients reflect relative balance between endo- and epicardial velocities and multilayer analysis reveals absolute values of myocardial velocities corresponding to endocardium and epicardium (Fig. 3).

Clinical Applications of Color M-Mode DTI

Normal Aging. Multilayer myocardial velocities and MVG in healthy patients demonstrate progressive changes with age in diastole, whereas no significant age-related changes have been reported in systolic peak velocities. These diastolic functional changes are related to the delayed ventricular relaxation observed in the elderly. With age, the peak velocity gradient decreases during ventricular filling and increases during atrial contraction (Fig. 4).²⁵ Multilayer analysis revealed that in early diastole the decrease in the endocardial velocities with age is more pronounced than that

in meso- and epicardial velocities. In contrast, in late diastole, the effects of age are similar in all layers. A progressive increase in endo-, meso-, and epicardial myocardial velocities is observed in elderly patients in telediastole.²⁶ These findings could be the functional correlate of anatomic findings in experimental models, indicating progressive myocardial cell loss and replacement fibrosis, which takes place mainly in the subendocardium.²⁷

Cardiomyopathies. Palka and colleagues²⁸ observed that peak systolic and protodiastolic MVG were lower in patients with hypertrophic cardiomyopathy than in athletes, hypertensive patients, or normal patients. It was also reported that peak protodiastolic MVG could accurately discriminate between hypertrophic cardiomyopathy and left ventricular hypertrophy in athletes.²⁸ Color M-mode DTI has also been used for the differential diagnosis between restrictive cardiomyopathy and constrictive pericarditis. Protodiastolic MVG measured from the LV posterior wall was significantly

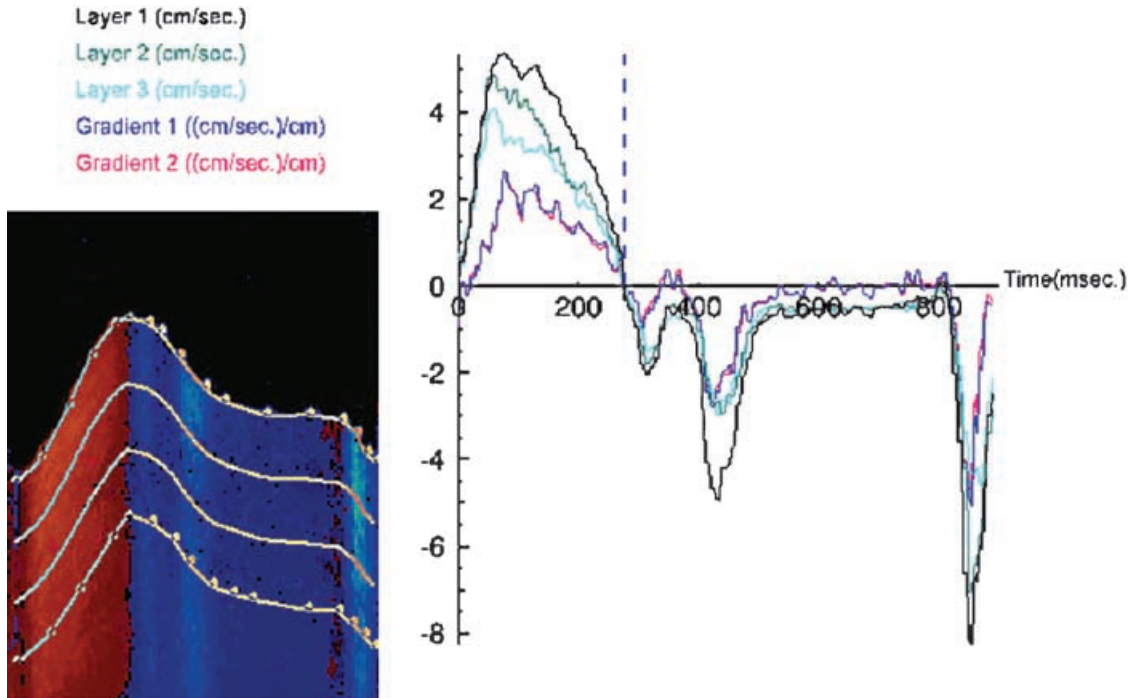


Figure 4. Color M-mode multilayer Doppler tissue imaging obtained in a healthy 85-year-old volunteer (left). Note the age-related differences in diastolic patterns compared with the younger volunteer in Figure 3. Interestingly, the effects of age in protodiastole are more pronounced in the subendocardium, whereas the changes in telediastole are more homogeneous across the myocardial wall.

lower in patients with restrictive cardiomyopathy compared with normal subjects and patients with constrictive pericarditis. Additionally, abnormal MVG during isovolumic relaxation was observed in patients with restrictive cardiomyopathy (positive MVG during isovolumic relaxation time) compared with patients with constrictive pericarditis and normal patients.²⁹ Color M-mode DTI has also been used for other purposes, such as the early detection of Duchenne's disease.³⁰

Ischemic Heart Disease. Previous studies have demonstrated that regional ischemic damage to the myocardium is heterogeneous in both spatial and temporal dimensions.³¹ This feature makes ischemic heart disease an ideal scenario for a detailed analysis of intramyocardial function with color M-mode DTI. Derumeaux et al.³² used color M-mode DTI in an experimental model of induced ischemia and found that acute ischemia reduced the gradient between endo- and epicardial velocities. Color M-mode DTI can also be helpful in studying myocardial recovery after reperfusion. A significant increase in peak systolic MVG has been observed after reperfusion in experimental nontransmu-

ral myocardial infarction, whereas transmural infarction did not have such an effect.³³

Garot and coworkers³⁴ reported that systolic and diastolic MVG are good indicators of contractility defects in ischemic segments. Furthermore, our group studied patients with ischemic heart disease and age-matched normal patients, and demonstrated that protodiastolic peak MVG can predict the presence of ischemia.³⁵ We also tested the utility of color M-mode multilayer analysis to assess the impact of ischemic damage on different myocardial layers in a group of patients with posterior myocardial infarction.³⁶ Peak systolic endo- and mesocardial velocities, as well as peak protodiastolic endocardial velocity, were significantly reduced in myocardial infarction compared with normal patients. Conversely, epicardial peak velocity was not significantly reduced, suggesting that less damage is produced by ischemia in the subepicardial fibers, as has been previously demonstrated by necropsy.³⁷

Tsutsui and colleagues³⁸ reported a higher accuracy of peak systolic MVG compared with visual interpretation of wall motion abnormalities for the detection of ischemic segments

during dobutamine stress testing. Therefore, it has been suggested that intramyocardial wall motion analysis could be useful for the early detection of ischemia and myocardial viability during dobutamine stress echocardiography. Further clinical studies are warranted to clarify the role of this modality in the stress test setting.

Strain and Strain Rate Imaging

Tissue velocities per se do not discriminate between actively contracting muscle and passive motion due to heart translation and tethering effects. In order to separate these two types of motion, "strain" and "strain rate" have been proposed as measures of regional contractility. Strain reflects the relative tissue deformation caused by an applied force or stress. It can be defined as the percent change in dimension from a resting state (L_0) to a new state (L) reached after the force was applied:

$$\varepsilon_L(t) = \int_{L_0}^L \frac{dL(t)}{L_0} = \frac{L(t) - L_0}{L_0}$$

This deformation could be positive or negative. In the case of myocardium, it corresponds to wall thickening or thinning in the radial direction. "Strain rate" is the rate of this relative deformation:

$$SR = \frac{d\varepsilon}{dt}$$

It can be measured indirectly as velocity difference divided by the distance between two points:

$$SR \approx \frac{v_1(t) - v_2(t)}{L(t)}$$

Using this definition, strain rate images (SRI) can be generated and strain can be calculated as the time integral of strain rate.

Strain and Strain Rate During Myocardial Ischemia

Greenberg and coworkers³⁹ demonstrated that peak and mean systolic strain rate are powerful noninvasive indices of LV contractility and are more consistent than peak systolic DTI velocities, possibly as a result of eliminating translation error. The ability of Doppler echocardiography to measure myocardial strain in a clinical setting demonstrated an excellent

correlation with the strains calculated by magnetic resonance imaging ($r = 0.89$ and $r = 0.96$ for longitudinal and radial strains, respectively, $P < 0.001$).⁴⁰

A first attempt to evaluate the clinical applicability of SRI for the assessment of regional LV function was made by Sutherland and coworkers,⁴¹ who studied patients with chronic transmural infarction and normal volunteers.⁴² They found that myocardial wall segments scored as hypokinetic, akinetic, and dyskinetic characterized typical and reproducible changes in the strain rate patterns. In hypokinetic and akinetic segments, shortening during isovolumic contraction was replaced by a positive lengthening wave. In systole, the onset of segmental shortening was delayed, and the peak systolic strain rate and strain decreased significantly with segmental asynergy. Not only could systolic strain and strain rate accurately identify infarct-involved segments,⁴² but also these parameters were significantly altered in normokinetic segments supplied by a coronary artery with a significant stenosis ($>70\%$) in comparison with control segments. Furthermore, velocities were found to be less specific in this setting because they were decreased not only in asynergic segments but also in the remote and well-perfused myocardium due to alteration in global LV function or tethering to adjacent ischemic segments. The systolic strain and strain rate had higher diagnostic accuracy (sensitivity 75% and 80%, specificity 80% and 82%, respectively) than systolic DTI velocities alone (sensitivity 68%, specificity 65%) for identifying acute ischemia.⁴³

SRI in Stress Echocardiography

Strain rate imaging can be used to evaluate myocardial function and accurately diagnose ischemia and assess viability in a clinical setting (Fig. 5). Several centers have demonstrated changes in regional myocardial velocity in response to stress and have successfully correlated these changes with normal, ischemic and scar responses. SRI is a more local measure of contractility, which is less affected by tethering. Both DTI systolic velocities and peak systolic strain increase with dobutamine in normally perfused segments and decrease in ischemic segments, but peak systolic strain appears to be affected by ischemia earlier.⁴⁴

Hoffmann and associates⁴⁵ analyzed 192 myocardial dyssynergic segments with SRI, at rest and after infusion of low doses of dobutamine.

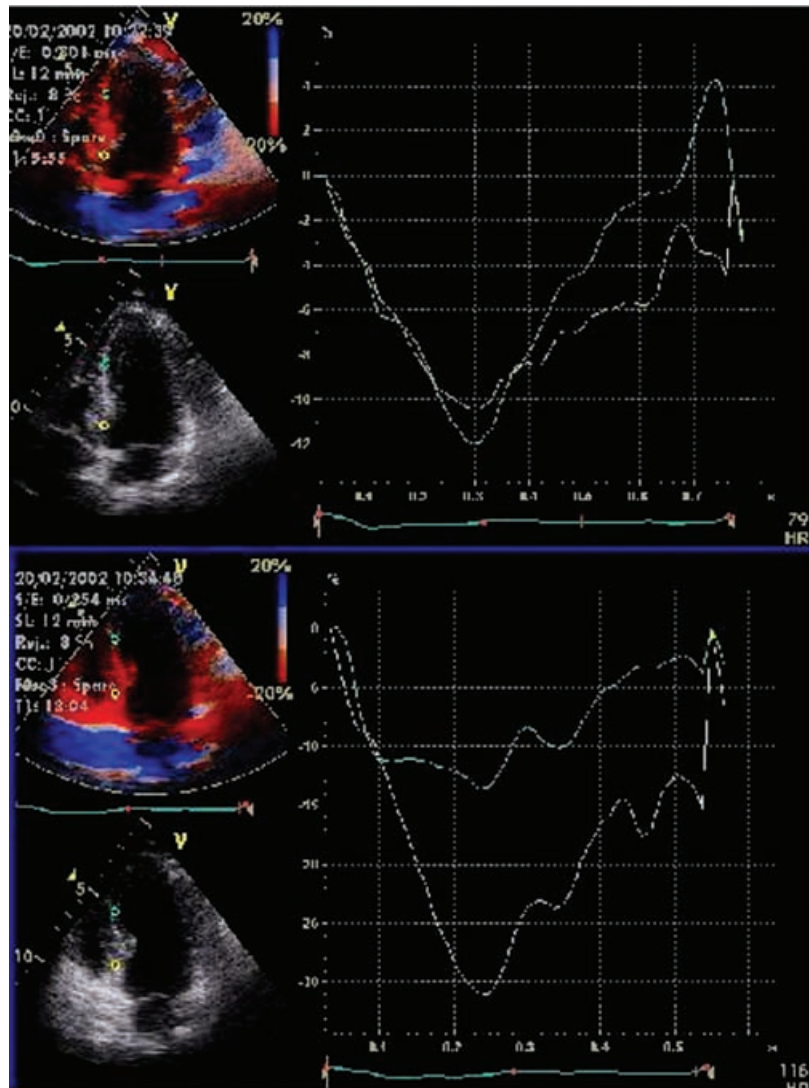


Figure 5. Compared with the strain rate profile obtained at rest in the basal and mid-septal segments (top), and at peak dose of dobutamine (bottom), the basal segment reveals a normal response with an increase in peak systolic strain of 20 units (from -10% to -30%). In the severely ischemic mid-septal segment, peak systolic strain increased from -20% to -12% . (Courtesy of A. Evangelista, M.D.)

Of the 192 segments, 94 were classified as viable and 98 nonviable by ^{18}F -fluorodeoxyglucose positron emission tomography (^{18}F FDG PET). In 83% of segments, dobutamine SRI assessment of viability was in agreement with PET, yielding sensitivity of 75% and specificity of 63%. An increase in peak systolic strain rate from rest to dobutamine by more than 0.23 s^{-1} allowed accurate discrimination of viable from nonviable myocardium with sensitivity of 83% and specificity of 84%.

Strain Rate in Resynchronization Therapy

Cardiac resynchronization therapy (CRT) is a promising therapeutic option in patients with severe heart failure and LBBB. With the use of DTI for the detection and quantification of

LV systolic performance and asynchrony, it was found that the extent of delayed longitudinal contraction (DLC) predicted the improvement in LV systolic performance during CRT. Strain rate analysis allows a better segmental location of DLC, represented by a negative strain rate wave during isovolumic relaxation time. In patients with idiopathic dilated cardiomyopathy, myocardium with DLC tended to be located in the lateral and posterior walls of the LV. In contrast, DLC was more frequent in the septum and in the inferior wall in patients with ischemic cardiomyopathy. With the recent development in pacemaker technology that allows separate activation of the ventricular leads, the information provided by SRI allows tailoring sequential CRT. Sogaard et al.⁴⁶ demonstrated

that compared with simultaneous CRT, tailored sequential CRT provides a significant improvement in LV performance.

Limitation of Strain and SRI

Strain and strain rate obtained from DTI have the intrinsic limitation of Doppler velocities: they are projections of the true three-dimensional velocity vector along the ultrasound scan line. Thus, strain rate images are only meaningful for wall segments where the deformation is parallel to the scan line, although significant errors occur when the angle between the true motion and the scan line is above 20 degrees. Another limitation is that only one strain/strain rate component is obtained, which limits the practical use of the method to the detection of segment shortening or lengthening in the longitudinal direction (apical view). An additional drawback is that the calculation of gradients is very sensitive to noise. Strain rate images, computed as differences between velocities in different spatial positions, exhibit low signal-to-noise ratios. The use of interpolation techniques, such as cubic spline,⁴⁷ has been proposed to overcome this problem. Nevertheless, poor definition of myocardial wall boundaries and noise present in Doppler signals make strain/strain rate images highly noisy.

Another consequence of the limited signal-to-noise ratio is low spatial resolution. Most reported studies use two points separated by 1 cm when computing the strain rate, after applying spatial and temporal filters. Studies performed in mathematical phantoms reported that resolutions better than 5 mm cannot be achieved with this method at the typical noise levels.

Automated Analysis of Regional Wall Motion

Attempts to automatically quantify endocardial excursion have been made since shortly after the introduction of two-dimensional echocardiography. However, primitive postprocessing mathematical algorithms and, more importantly, poor image quality precluded using these systems in the clinical setting.

Integrated Backscatter Based Methods

During the early 1990s the development of integrated backscatter imaging modalities allowed a major enhancement of the blood-

endocardium interface.^{48,49} Acoustic quantification represented the first system that provided reproducible and accurate online parameters of global LV systolic and diastolic function. A few years later color kinesis allowed both enhanced visualization and objective measurement of regional endocardial excursion.⁵⁰⁻⁵³ Although these systems never gained widespread use in everyday clinical practice, their merit as pioneer methods for quantitative analysis of ventricular wall motion should be noted. Clinical studies performed using color kinesis reported that quantitative methods can improve the diagnostic accuracy of subjective echocardiography in the diagnosis of ischemic heart disease.⁵⁰⁻⁵³

Recent development of tissue harmonic imaging has represented a gigantic step forward in the quality of two-dimensional echocardiographic images.⁵⁴ Although endocardial border detection based on acoustic quantification has significantly benefited from this development,⁵⁵ new nonlinear harmonic imaging modes combined with second-generation intravenous contrast agents provided an even more dramatic improvement in LV opacification and endocardial definition. Endocardial border can now be clearly depicted in practically all echocardiographic views in the vast majority of patients referred for echocardiographic examination. Acoustic quantification software has been recently modified to detect and track the endocardial boundary on contrast-enhanced image sequences, and initial clinical studies using this system are encouraging.⁵⁶⁻⁵⁸

Methods Based on B-Mode Endocardial Tracking

Digital postprocessing imaging techniques have evolved during recent years so much that they have become an integral part of nuclear medicine, magnetic resonance imaging, and computed tomography. Feature-extraction algorithms are now capable of providing automatic recognition of anatomic structures in these imaging modalities. Today these artificial-vision based techniques are being introduced into the field of cardiac ultrasound.

Briefly, these systems are based on two sources of input: image data and "a priori" knowledge. Raw image data from digitally stored ultrasound sequences are processed using complex digital filtering and intensity normalization algorithms aimed at enhancing the

endocardial boundary. This initial phase in endocardial tracking is designated image segmentation or feature enhancement. The second step is the incorporation of prespecified intelligence, such as the knowledge of LV cavity size and shape, as well as notions of temporal and spatial endocardial motion. Thus, the endocardial contour is first defined using mathematical spline and snake functions based on initial input provided by the user for one image at the beginning of the sequence. Then the system deforms this initial contour according to image data in the next frame and the a priori knowledge. Once the whole image sequence is tracked, quantitative parameters of global and regional function are obtained (Figs. 5 and 6).⁵⁹⁻⁶³

This type of system offers a number of advantages. First, accuracy is increased because noise artifacts and shadowing are markedly reduced. Second, local correspondences among all local

points in the contour are preserved, which ensures that regional analysis can be performed accurately. Third, individual contour position in time and space is calculated and can be combined in a three-dimensional volume.

We have recently participated in the development and clinical validation of one of these tracking systems using acoustic quantification with harmonic contrast images sequences as initial input.^{59,63} Our results demonstrated that the system is as accurate as visual analysis of LV function with the advantage of increased reproducibility. We also tested the system for the analysis of LV contrast echocardiograms obtained during dobutamine stress testing, and found that quantitative parameters of regional excursion closely correlated with visual scoring of regional wall motion. Whether this tool finally increases the diagnostic accuracy of stress echocardiography remains to be ascertained in future studies.

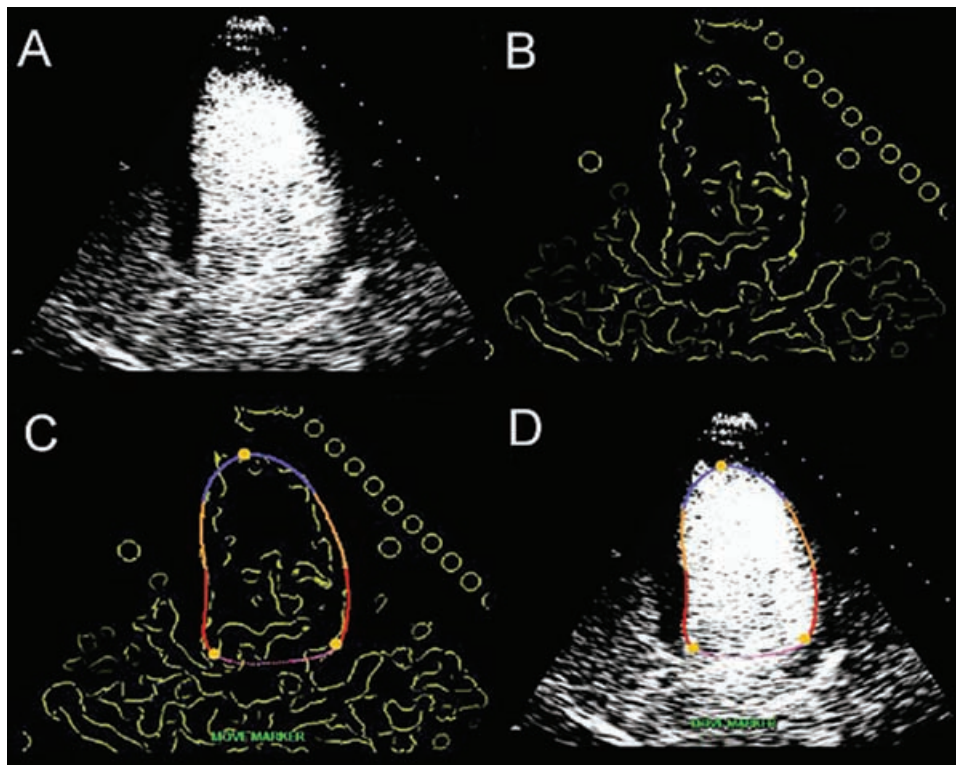


Figure 6. Endocardial tracking of a contrast-enhanced two-dimensional image sequence. (A) A raw image is subjected to segmentation and feature extraction using (B) intensity equalization and filtering, followed by (C) spline fitting of the endocardial contour incorporating knowledge of left ventricular shape, size, and endocardial displacement. (D) The extracted endocardial boundary is overlaid on the original image to check result accuracy and to correct potential errors.

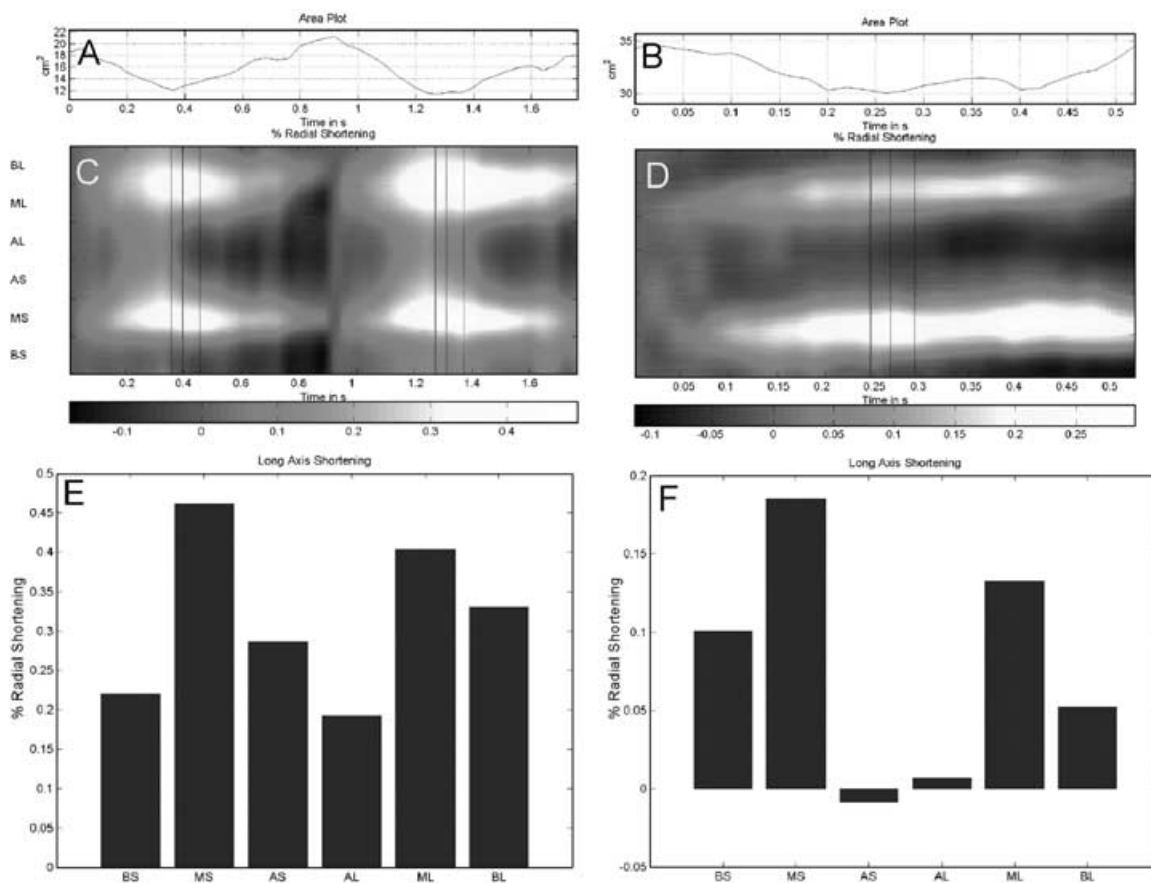


Figure 7. Quantitative analysis of left ventricular motion from a normal patient (panels A, C, and E illustrate two cardiac cycles), and from a patient with an apical myocardial infarction (panels B, D, and F illustrate one cardiac cycle). Plots are the results of processing instantaneous contours obtained from an apical four-chamber view. (A and B) Illustration of instantaneous values of global area. (C and D) Illustration of a quantitative display of regional shortening. The horizontal axis represents time, matched to panels A and B. The vertical axis represents each point along the contour in the clockwise sequence: basal-septum (BS), mid-septum (MS), apical-septum (AS), apical-lateral (AL), mid-lateral (ML), and basal-lateral (BL). The color scale represents the percent of radial shortening for each point in the contour. Notice that using this display the differences in the amount and timing of border excursion are readily displayed. (E and F) Histograms depicting long-axis shortening for each segment.

Image Intensity Tracking Based on B-Mode Endocardial Tracking

Intensity-based methods have a great potential for providing myocardial strain in every point in the myocardium as previously proposed for magnetic resonance image sequences.^{64–67} The aim of these methods is to detect the displacement of every anatomic point by searching for correspondence between the intensity of pixels within the myocardium along the image cycle. This is commonly referred to as “dense displacement field” and provides a displacement vector for every point in the myocardium, whereas border tracking methods only provide

displacement vectors for points along the endocardial border. Therefore, border tracking methods can only assess endocardial motion, while no information about myocardial thickening or intramyocardial functionality can be obtained. The dense cardiac displacement, on the other hand, allows examining of multiple parameters of myocardial dynamics.

Two different approaches have been proposed to compute the dense cardiac displacement field. The first approach tracks local intensity in a pixel-by-pixel basis (or small neighborhoods), finding correspondences at a local level. Among these techniques, the most characteristic are optical flow methods and block matching

methods. To avoid large changes in the displacement amplitude or direction from frame to frame, some kind of global smoothness constraint is usually added to impose spatial coherence in the displacement field.⁶⁸

The second approach retrieves the dense displacement field by calculating the deformation between every pair of images so that one of the images is deformed to be as similar as possible to the other. This process is commonly referred to as alignment or registration. The deformation computed for one pair of images provides an incremental displacement. The alignment process is repeated for all consecutive pairs of images in the sequence along the cardiac cycle (Fig. 7). Incremental displacements are added together to compute the trajectory, defined as the accumulated displacement for every point in the image.^{69,70} The deformation between a pair of images is obtained iteratively, by minimizing the difference in intensity between the two images, while adjusting the deformation parameters. The deformation must be elastic or nonrigid due to the elastic nature of the myocardium. These methods take into account all pixels in the image in a global manner, computing all displacements at the same time. The smoothness and spatial coherence is therefore automatically imposed within the deformation definition. Figure 8 illustrates an example of the dense displacement field obtained in a patient with hypokinetic function of the lateral wall as web, basal, and distal septum segments. Thorough validation of these techniques is required to establish their potential role in the clinical echocardiographic assessment of LV function.

Four-Dimensional Endocardial Tracking

Four-dimensional (or dynamic three-dimensional) echocardiography is rapidly evolving and a variety of systems are capable of obtaining volumetric image datasets. However, quantitative parameters of global and regional wall motion can only be obtained after endocardial boundary recognition and tracking is performed. A number of attempts have been taken in this direction.⁷¹⁻⁷³ We have recently evaluated a prototype system for surface rendering from four-dimensional harmonic contrast echocardiographic datasets based on the tracking system described above, and we found instantaneous ventricular volumes estimates made by this system to be accurate.⁷⁴

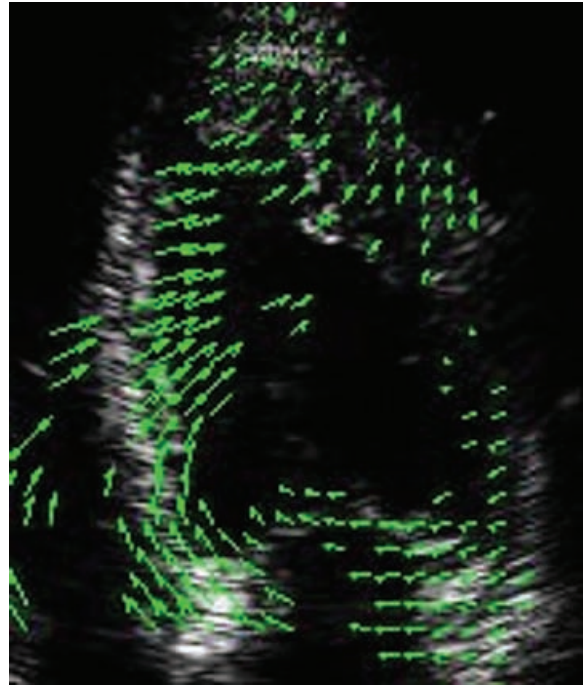


Figure 8. Alignment of consecutive pairs of images allows the computation of incremental displacements and the trajectory of every point in the image. Image was obtained from a patient with hypokinetic function of the lateral wall, and the basal and distal septum segments are illustrated with the dense myocardial displacement field.

Methods Based on Tissue Doppler Tracking

Myocardial velocity information provided by color tissue Doppler can be used to track the endocardial boundary. Instantaneous temporal integration of the velocity data of a given image pixel equals spatial position. On this basis some ultrasound scanners are capable of providing online endocardial tracking, and initial clinical applications of this approach have been described.⁷⁵⁻⁷⁷ Optimization of these systems will likely include combining the velocity information with B-mode data processing algorithms discussed above.

References

1. Fukuda K, Oki T, Tabata T, et al: Regional left ventricular wall motion abnormalities in myocardial infarction and mitral annular descendent velocities studied with pulsed tissue Doppler imaging. *J Am Soc Echocardiogr* 1998;11:841-848.
2. Onose Y, Oki T, Mishiro Y, et al: Influence of aging on systolic left ventricular wall motion velocities along the long and short axes in clinically normal patients determined by pulsed tissue Doppler imaging. *J Am Soc Echocardiogr* 1999;12:921-926.

3. Mishiro Y, Oki T, Yamada H, et al: Evaluation of left ventricular contraction abnormalities in patients with dilated cardiomyopathy with the use of pulsed tissue Doppler imaging. *J Am Soc Echocardiogr* 1999;12:913–920.
4. Oki T, Iuchi A, Tabata T, Mishiro Y, et al: Left ventricular systolic wall motion velocities along the long and short axes measured by pulsed tissue Doppler imaging in patients with atrial fibrillation. *J Am Soc Echocardiogr* 1999;12:121–128.
5. Koyama J, Ray-Sequin PA, Davidoff R, et al: Usefulness of pulsed tissue Doppler imaging for evaluating systolic and diastolic left ventricular function in patients with AL (primary) amyloidosis. *Am J Cardiol* 2002;89:1067–1071.
6. Vinereanu D, Florescu N, Sculthorpe N, et al: Differentiation between pathologic and physiologic left ventricular hypertrophy by tissue Doppler assessment of long-axis function in patients with hypertrophic cardiomyopathy or systemic hypertension and in athletes. *Am J Card* 2001;88:53–58.
7. D'Andrea A, Caso P, Severino S, et al: Effects of different training protocols on left ventricular myocardial function in competitive athletes: A Doppler tissue imaging study. *Ital Heart J* 2002;3:34–40.
8. Zoncu S, Pelliccia A, Mercurio G: Assessment of regional systolic and diastolic wall motion velocities in highly trained athletes by pulsed wave Doppler tissue imaging. *J Am Soc Echocardiogr* 2002;15:900–905.
9. Yamada E, Garcia M, Thomas JD, et al: Myocardial Doppler velocity imaging—A quantitative technique for interpretation of dobutamine echocardiography. *Am J Cardiol* 2001;87:525–531.
10. Altinmakas S, Dagdeviren B, Uyan C, et al: Prediction of viability by pulsed-wave Doppler tissue sampling of asynergic myocardium during low-dose dobutamine challenge. *Int J Cardiol* 2000;74:107–113.
11. D'Andrea A, Caso P, Galderisi M, et al: Ventricular interdependence in patients with dual-chamber pacing: A Doppler tissue imaging study. *Echocardiography* 2002;19:289–297.
12. Yu CM, Chau E, Sanderson JE, et al: Tissue Doppler echocardiographic evidence of reverse remodeling and improved synchronicity by simultaneously delaying regional contraction after biventricular pacing therapy in heart failure. *Circulation* 2002;105:438–445.
13. Sogaard P, Egeblad H, Kim WY, et al: Tissue Doppler imaging predicts improved systolic performance and reversed left ventricular remodeling during long-term cardiac resynchronization therapy. *J Am Coll Cardiol* 2002;40:723–730.
14. Garcia Fernández MA, Zamoano J, Acevedo R, et al: Doppler tissue imaging limitation In: *Doppler tissue imaging echocardiography*. Mc Graw-Hill, 1998, pp. 133–141.
15. Sabbah HN, Marzilli M, Stein PD: The relative role of subendocardium and subepicardium in left ventricle mechanics. *Am J Physiol* 1981;240:H920–H926.
16. Gallagher KP, Osakada G, Matsuzaki M, et al: Nonuniformity of inner and outer systolic wall thickening in conscious dogs. *Am J Physiol* 1985;249:H241–H248.
17. Derumeaux G, Ovize M, Loufoua J, et al: Assessment of nonuniformity of transmural myocardial velocity by color-coded tissue Doppler imaging: Characterization of normal, ischemic, and stunned myocardium. *Circulation* 2000;101:1390–1395.
18. Arts T, Reneman RS, Veenstra PC: A model of the mechanics of the left ventricle. *Ann Biomed Eng* 1979;7:299–318.
19. Rijcken J, Bovendeerd PH, Schoofs AL, et al: Optimization of cardiac fiber orientation for homogeneous fiber strain during ejection. *Ann Biomed Eng* 1999;27:289–297.
20. Garot J, Diebold B, Derumeaux G, et al: Comparison of regional myocardial velocities assessed by quantitative 2-dimensional and M-mode color Doppler tissue imaging: Influence of the signal-to-noise ratio of color Doppler myocardial images on velocity estimators of the Doppler tissue imaging system. *J Am Soc Echocardiogr* 1998;11:1093–1105.
21. Uematsu M, Miyatake K, Tanaka N, et al: Myocardial velocity gradient as a new indicator of regional left ventricular contraction: Detection by a two-dimensional tissue Doppler imaging technique. *J Am Coll Cardiol* 1995;26:217–223.
22. Fleming A, Xia X, McDicken W, et al: Myocardial velocity gradients detected by Doppler imaging system. *Br J Radiol* 1994;67:679–688.
23. Desco M, Antoranz JC: Technical principles of Doppler tissue imaging. In: García-Fernández MA, Zamorano J, Azevedo J (eds.): *Doppler Tissue Imaging Echocardiography*. New York: Mc Graw Hill, 1998, pp. 7–23.
24. Zamorano J, Wallbridge D, Ge J, et al: Non-invasive assessment of cardiac physiology by tissue Doppler echocardiography. *Eur Heart J* 1997;18:330–339.
25. Palka P, Lange A, Fleming AD, et al: Age-related transmural peak mean velocities and peak velocity gradients by Doppler myocardial imaging in normal subjects. *Eur Heart J* 1996;17:940–950.
26. Perez-David E, García-Fernández MA, Ledesma MJ, et al: Age-related intramyocardial function patterns. (Abstract) *Circulation* 2002;106:397.
27. Anversa P, Hiler B, Ricci R, et al: Myocyte cell loss and myocyte hypertrophy in the aging rat heart. *J Am Coll Cardiol* 1986;8:1441–1448.
28. Palka P, Lange A, Fleming AD, et al: Differences in myocardial velocity gradient measured throughout the cardiac cycle in patients with hypertrophic cardiomyopathy, athletes and patients with left ventricular hypertrophy due to hypertension. *J Am Coll Cardiol* 1997;30:760–768.
29. Palka P, Lange A, Donnelly JE, et al: Differentiation between restrictive cardiomyopathy and constrictive pericarditis by early diastolic Doppler myocardial velocity gradient at the posterior wall. *Circulation* 2000;102:655–662.
30. Chetboul V, Escriou C, Thibaud JL, et al: Antenatal detection of Duchenne's cardiomyopathy by tissue Doppler. (Abstract) *Circulation* 2002;106:397.
31. Gallagher KP, Stirling MC, Choy M, et al: Dissociation between epicardial and transmural function during acute myocardial ischemia. *Circulation* 1985;71:1279–1291.
32. Derumeaux G, Ovize M, Loufoua J, et al: Assessment of nonuniformity of transmural myocardial velocity by color-coded tissue Doppler imaging: Characterization of normal, ischemic, and stunned myocardium. *Circulation* 2000;101:1390–1395.
33. Derumeaux G, Loufoua J, Pontier G, et al: Tissue Doppler imaging differentiates transmural from non transmural acute myocardial infarction after reperfusion therapy. *Circulation* 2001;103:589–596.
34. Garot J, Derumeaux GA, Monin JL, et al: Quantitative systolic and diastolic transmyocardial velocity

- gradients assessed by M-mode colour Doppler tissue imaging as reliable indicators of regional left ventricular function after acute myocardial infarction. *Eur Heart J* 1999;20:593–603.
35. Desco M, Ledesma MJ, Pérez-David E, et al: Assessment of normal and ischaemic myocardium by quantitative M-mode Doppler Tissue Imaging. *Ultrasound Med Biol* 2002;28:561–569.
 36. Marcos-Alberca P, García Fernández MA, Ledesma MJ, et al: Intramyocardial analysis of regional systolic and diastolic function in ischemic heart disease with Doppler tissue imaging: role of the different myocardial layers. *J Am Soc Echocardiogr* 2002;15:99–108.
 37. Jones C, Raposo L, Gibson D: Functional importance of the long axis dynamics of the human left ventricle. *Br Heart J* 1990;63:215–220.
 38. Tsutsui H, Uematsu M, Shimizu H, et al: Comparative usefulness of myocardial velocity gradient in detecting ischemic myocardium by a dobutamine challenge. *J Am Coll Cardiol* 1998;31:89–93.
 39. Greenberg NL, Firstenberg MS, Castro PL, et al: Doppler-derived myocardial systolic strain rate is a strong index of left ventricular contractility. *Circulation* 2002;105:99–105.
 40. Edvardsen T, Gerber BL, Garot J, et al: Quantitative assessment of intrinsic regional myocardial deformation by Doppler strain rate echocardiography in humans. Validation against three-dimensional tagged magnetic resonance imaging. *Circulation* 2002;106:50–56.
 41. Sutherland GR, Kukulski T, Voight JU, et al: Tissue Doppler echocardiography. Future developments. *Echocardiography* 1999;16:509–520.
 42. Jamal F, Kukulski T, Sutherland GR, et al: Can changes in systolic longitudinal deformation quantify regional myocardial function after an acute infarction? An ultrasonic strain rate and strain study. *J Am Soc Echocardiogr* 2002;15:723–730.
 43. Kukulski T, Jamal F, D'Hooge J, et al: Acute changes in systolic and diastolic events during clinical coronary angioplasty a comparison of regional velocity, strain rate and strain measurement. *J Am Soc Echocardiogr* 2002;15:1–12.
 44. Armstrong G, Pasquet A, Fukamachi K, et al: Use of peak systolic strain as an index of regional left ventricular function: Comparison with tissue Doppler velocity during dobutamine stress and myocardial ischemia. *J Am Soc Echocardiogr* 2000;13:731–737.
 45. Hoffmann R, Altoik E, Nowak B, et al: Strain rate measurement by Doppler echocardiography allows improved assessment of myocardial viability in patients with depressed left ventricular function. *J Am Coll Cardiol* 2002;39:443–449.
 46. Sogaard P, Egeblad H, Pedersen AK, et al: Sequential versus simultaneous biventricular resynchronization for severe heart failure. Evaluation by tissue Doppler imaging. *Circulation* 2002;106:2078–2084.
 47. Santos A, Ledesma-Carbayo MJ, Malpica N, et al: Accuracy of heart strain rate calculation derived from Doppler tissue velocity data. In Insana MF, Shug KK (eds.): *SPIE Proc Medical Imaging* 2001;4325:546–556.
 48. Perez JE, Klein SC, Prater DM, et al: Automated, on-line quantification of left ventricular dimensions and function by echocardiography with backscatter imaging and lateral gain compensation. *Am J Cardiol* 1992;70:1200–1205.
 49. Perez JE, Waggoner AD, Barzilai B, et al: On-line assessment of ventricular function by automatic boundary detection and ultrasonic backscatter imaging. *J Am Coll Cardiol* 1992;19:313–320.
 50. Mor-Avi V, Vignon P, Koch R, et al: Segmental analysis of color kinesis images: New method for quantification of the magnitude and timing of endocardial motion during left ventricular systole and diastole. *Circulation* 1997;95:2082–2097.
 51. Lang RM, Vignon P, Weinert L, et al: Echocardiographic quantification of regional left ventricular wall motion with color kinesis. *Circulation* 1996;93:1877–1885.
 52. Vignon P, Mor-Avi V, Weinert L, et al: Quantitative evaluation of global and regional left ventricular diastolic function with color kinesis. *Circulation* 1998;97:1053–1061.
 53. Carey CF, Mor-Avi V, Koch R, et al: Effects of inotropic stimulation on segmental left ventricular relaxation quantified by color kinesis. *Am J Cardiol* 2000;85:1476–1480.
 54. Caidahl K, Kazzam E, Lidberg J, et al: New concept in echocardiography: harmonic imaging of tissue without use of contrast agent. *Lancet* 1998;352:1264–1270.
 55. Tsujita-Kuroda Y, Zhang G, Sumita Y, et al: Validity and reproducibility of echocardiographic measurement of left ventricular ejection fraction by acoustic quantification with tissue harmonic imaging technique. *J Am Soc Echocardiogr* 2000;13:300–305.
 56. Mor-Avi V, Caiani EG, Collins KA, et al: Combined assessment of myocardial perfusion and regional left ventricular function by analysis of contrast-enhanced power modulation images. *Circulation* 2001;104:352–357.
 57. Mor-Avi V, Bednarz J, Weinert L, et al: Power Doppler imaging as a basis for automated endocardial border detection during left ventricular contrast enhancement. *Echocardiography* 2000;17:529–537.
 58. Spencer KT, Bednarz J, Mor-Avi V, et al: Automated endocardial border detection and evaluation of left ventricular function from contrast-enhanced images using modified acoustic quantification. *J Am Soc Echocardiogr* 2002;15:777–781.
 59. Bermejo J, Mulet M, Moreyra C, et al: Endocardial tracking of acoustic quantification and contrast power-Doppler echocardiographic images: Clinical validation against cine-MRI and manual segmentation. (Abstract) *Circulation* 1999;100:326.
 60. Jacob G, Noble JA, Kelion AD, et al: Quantitative regional analysis of myocardial wall motion. *Ultrasound Med Biol* 2001;27:773–784.
 61. Jacob G, Noble JA, Mulet-Parada M, et al: Evaluating a robust contour tracker on echocardiographic sequences. *Med Image Analysis* 1999;3:63–75.
 62. Jacob G, Noble JA, Behrenbruch C, et al: A shape-space-based approach to tracking myocardial borders and quantifying regional left-ventricular function applied in echocardiography. *IEEE Trans Med Imaging* 2002;21:226–238.
 63. Nurbekov Y, Bermejo J, Mulet-Parada M, et al: Endocardial tracking from two-dimensional integrated-backscatter echocardiographic sequences. Initial validation against manual segmentation and cine-MRI. (Abstract) *Circulation* 2001;104:653.
 64. Clarysse P, Basset C, Khouas L, et al: Two-dimensional spatial and temporal displacement and

- deformation field fitting from cardiac magnetic resonance tagging. *Med Image Analysis* 2000;4:253–268.
65. McEachen JC, Nehorai A, Duncan JS: Multiframe temporal estimation of cardiac non-rigid motion. *IEEE Trans Med Imaging* 2000;9:651–664.
 66. Shi P, Sinusas AJ, Constable RT, et al: Volumetric deformation analysis using mechanics-based data fusion: Applications in cardiac motion recovery. *Int J Computer Vision* 1999;35:87–107.
 67. Jacob G, Noble A, Mulet-Parada M, et al: Evaluating a robust contour tracker on echocardiographic sequences. *Med Image Analysis* 1999;3:63–75.
 68. Yeung F, Levinson F, Fu D, et al: Feature-adaptive motion tracking of ultrasound image sequences using a deformable mesh. *IEEE Trans Med Imaging* 1998;17:945–956.
 69. Ledesma-Carbayo MJ, Kybic J, Desco M, et al: Cardiac motion analysis from ultrasound sequences using non-rigid registration. In Niessen WJ, Viergeber MA (eds.): *Lecture Notes in Computer Science* (Volume 2208). Berlin: Springer Verlag, 2001, pp. 889–896.
 70. Ledesma-Carbayo MJ, Kybic J, Sühling M, et al: Cardiac ultrasound motion detection by elastic registration exploiting temporal coherence. *IEEE Int Symp Biomed Imaging* 2002;1:585–588.
 71. Papademetris X, Sinusas AJ, Dione DP, et al: Estimation of three-dimensional left ventricular deformation from echocardiography. *Med Image Analysis* 2001;5:17–28.
 72. Jiang L, Morrissey R, Handschumacher MD, et al: Quantitative three-dimensional reconstruction of left ventricular volume with complete borders detected by acoustic quantification underestimates volume. *Am Heart J* 1996;131:553–559.
 73. Chuang ML, Beaudin RA, Riley MF, et al: Impact of on-line endocardial border detection on determination of left ventricular volume and ejection fraction by transthoracic three-dimensional echocardiography. *J Am Soc Echocardiogr* 1999;12:551–558.
 74. Bermejo J, Lang R, Odreman R, et al: Four-dimensional surface tracking of contrast-enhanced transthoracic biplane echocardiograms: A new tool for quantitative assessment of LV function. (Abstract) *J Am Coll Cardiol* 2003;41 (Suppl A): 437A.
 75. Tanaka N, Tone T, Ono S, et al: Predominant inner-half wall thickening of left ventricle is attenuated in dilated cardiomyopathy: an application of tissue Doppler tracking technique. *J Am Soc Echocardiogr* 2001;14:97–103.
 76. Takenaka K, Kuwada Y, Sonoda M, et al: Anthracycline-induced cardiomyopathies evaluated by tissue Doppler tracking system and strain rate imaging. *J Cardiol* 2001;37:129–32.
 77. Pan C, Hoffmann R, Kuhl H, et al: Tissue tracking allows rapid and accurate visual evaluation of left ventricular function. *Eur J Echocardiogr* 2001;2:197–202.